European Journal of Medicinal Chemistry 48 (2012) 26–35

Contents lists available at SciVerse ScienceDirect

European Journal of Medicinal Chemistry

journal homepage: http://www.elsevier.com/locate/ejmech

Original article

Synthesis, structural characterization and *in vitro* biological screening of some homoleptic copper(II) complexes with substituted guanidines

Ghulam Murtaza [a], Muhammad Khawar Rauf [a], Amin Badshah [a,*], Masahiro Ebihara [c], Muhammad Said [a], Marcel Gielen [b], Dick de Vos [d], Erum Dilshad [e], Bushra Mirza [e]

[a] Department of Chemistry, Quaid-i-Azam University, Islamabad 45320, Pakistan
[b] Vrije Universiteit Brussel, Faculty of Engineering, HNMR Unit, 1050 Brussels, Belgium
[c] Department of Chemistry, Faculty of Engineering, Gifu University Yanagido, Gifu 501-1193, Japan
[d] Pharmachemie B.V., P.O. Box 552, 2003 RN, Haarlem, The Netherlands
[e] Department of Biochemistry, Faculty of Biological Sciences, Quaid-i-Azam University, Islamabad 45320, Pakistan

ARTICLE INFO

Article history:
Received 8 June 2011
Received in revised form
14 November 2011
Accepted 15 November 2011
Available online 1 December 2011

Keywords:
Copper(II) complexes
N,N′,N″-trisubstituted guanidines
Cytotoxicity
Crystal structures
Human cell lines

ABSTRACT

A series of homoleptic copper(II) complexes (**1a**–**8a**) with N,N′,N″-trisubstituted guanidines, [Cu(II){PhCONHC(NHR)NPh}$_2$] (where R = phenyl (**1a**), *n*-butyl (**2a**), *sec*-butyl (**3a**), cyclohexyl (**4a**), 1-naphthyl (**5a**), 2,4-dichlorophenyl (**6a**), 3,4-dichlorophenyl (**7a**), and 3,5-dichlorophenyl (**8a**)) have been synthesized and characterized by elemental analyses, FT-IR, UV–visible, ^{1}H and ^{13}C NMR spectroscopy, and single crystal X-ray diffraction analysis. The X-ray crystal structures revealed that the complexes **2a** and **4a** are mononuclear in the solid state and that the geometry around the copper atom is nearly square planar. In both the cases, N,N′,N″-trisubstituted guanidine ligands have been coordinated to the Cu(II) through the oxygen and nitrogen atoms. The synthesized guanidines and their complexes were initially screened for their anti-microbial activities, and Brine Shrimps Lethality assay. The complexes were also screened for *in vitro* cytotoxicity activity in human cell lines carcinomas A498, EVSAT, H226, IGROV, M19, MCF-7 and WIDR. The results show a moderate level of cytotoxicity against these seven human cancer cell lines as compared with standard chemotherapeutic drugs.

1. Introduction

One of the fundamental goals in medicinal chemistry is the development of new anticancer and anti-microbial therapeutic agents. Cancer treatment using metal-based drugs is one of the very effective strategies as the metal ions are capable of binding to nucleic acids stereo-specifically with varying strength [1–3]. Copper being an essential metal for animals and non-toxic in controlled quantity is implicated in many diseases [4]. The toxicity of metal atoms is due to those reactions of the redox-active metal ions which generate reactive oxygen species (ROS) that damage DNA and other biomolecules, probably *via* Haber-Weiss or Fenton-like reactions [5]. The accumulation of copper is observed to be a physiological feature of many tumor tissues and cells as was demonstrated in many types of human cancers including breast, prostate, colon, lung and brain [6–8]. However, there are several metal-organic compounds that actively and specifically inhibit the chymotrypsin like activity of the proteasome *in vitro* and in human tumor-cell cultures [9]. Copper(II) complexes have been extensively utilized in DNA cleavage for the generation of activated oxygen species by redox cycling properties between Cu(II) and Cu(I), presumably a hydroxyl radical, which can react at several nucleic acid sites to break it [10–12]. Copper(II) complexes with N and O donating ligands have also been studied for their nuclease properties [13,14]. The copper accumulates in tumors due to the selective permeability of the cancer cell membrane to copper compounds. For these reasons, a number of copper complexes have been screened for their anticancer activity and some of them were found active both *in vivo* and *in vitro* [15–17].

Guanidine functionalities are found in a variety of natural compounds, either in cyclic form, or as terminal groups of pendent substituents [18]. Some of the naturally occurring guanidines were screened for their nuclease activity and exhibit cytotoxic properties [19]. The guanidine group acts as an inhibitor of urokinase that

Abbreviations: DMSO, Dimethylsulphoxide; DMF, Dimethylformamide; TLC, Thin layer chromatography; SRB, Sulphorhodamine B; FCS, Fetal Calf Serum; PBS, Fetal Bovine Serum; RPMI, Roswell Park Memorial Institute; TCA, Trichloroacetic acid.

* Corresponding author.
E-mail addresses: mkhawarrauf@yahoo.co.uk (M.K. Rauf), aminbadshah@yahoo.com (A. Badshah).

0223-5234/$ – see front matter © 2011 Elsevier Masson SAS. All rights reserved.
doi:10.1016/j.ejmech.2011.11.029

plays a vital role in tumor metastasis and is implicated in a large number of malignancies, including breast, lungs, bladder, stomach, cervix, kidney, and brain cancers [20]. Various guanidine compounds have also been synthesized and tested for their anti-tumor activity [21,22]. The studies had revealed that polyaromatic guanidinium derivatives lengthen the DNA helix forming stronger complexes which confer cytotoxic activities [23].

Though the anticancer activity of different platinum and palladium metals appear to be promising, these metals are unnatural to the human body because there is no effective mechanism for their rejection as for the other metals like copper and iron. It is, therefore, an endeavor to find out the cytotoxic effects of copper(II) complexes. Herein, we report the synthesis of a series of copper(II) complexes of novel substituted acylguanidines with a view to design anticancer drugs that are more potent as well as friendly to the human body. As some reports demonstrated that copper complexes of guanidines also exhibit antibacterial and antifungal activities [24] that is enhanced by complexation with copper [15], so we are also presenting the bactericidal and fungicidal activities for the synthesized compounds.

2. Results and discussion

2.1. Chemistry

A series of guanidine ligands (**1**–**8**), N,N′-diphenyl-N"-benzoylguanidine (**1**), N-phenyl-N′-(*n*-butyl)-N″-benzoylguanidine (**2**), N-phenyl-N′-(sec-butyl)-N″-benzoylguanidine (**3**), N-phenyl-N′-cyclohexyl-N"-benzoylguanidine (**4**), N-phenyl-N′-(1-naphthyl)-N″-benzoylguanidine (**5**), N-phenyl-N′-(2,4-dichlorophenyl)-N″-benzoylguanidine (**6**), N-phenyl-N′-(3,4-dichlorophenyl)-N″-benzoylguanidine (**7**) and N-phenyl-N′-(3,5-dichlorophenyl)-N″-benzoylguanidine (**8**) were synthesized from N-benzoyl-N′-phenylthiourea by using a standard catalytic guanylation reaction method [25a]. By reacting these ligands with copper(II) acetate, a series of homoleptic complexes (**1a**–**8a**), bis(N,N′-diphenyl-N"-benzoylguanidinato)copper(II) (**1a**), bis(N-phenyl-N′-(*n*-butyl)-N″-benzoylguanidinato)copper(II) (**2a**), bis(N-phenyl-N′-(sec-butyl)-N″-benzoylguanidinato)copper(II) (**3a**), bis(N-phenyl-N′-cyclohexyl-N"-benzoylguanidinato)copper(II) (**4a**), bis(N-phenyl-N′-(1-naphthyl)-N″-benzoylguanidinato)copper(II) (**5a**), bis(N-phenyl-N′-(2,4-dichlorophenyl)-N″-benzoylguanidinato)copper(II) (**6a**), bis(N-phenyl-N′-(3,4-dichlorophenyl)-N″-benzoylguanidinato)copper(II) (**7a**) and bis(N-phenyl-N′-(3,5-dichlorophenyl)-N″-benzoylguanidinato)copper(II) (**8a**) were also synthesized. The purity of the ligands and complexes was checked by TLC with Merck Kieselgel GF 254 Plates, elemental analysis, ^{1}H- and ^{13}C-NMR (Bruker ARX, 300 MHz spectrometer).

2.2. Synthesis and spectroscopic studies

The entire polysubstituted guanidines and their Cu(II) complexes were synthesized in good yield, which were characterized by different analytical techniques. In FT-IR spectra of ligands two peaks, a sharp and other weak, were observed for N–H bonds in the range 3246–3393 cm^{-1}, except for **1** which have electronically similar environment for both N–H. The weak N–H band at longer wavelength may be attributed to the involvement of hydrogen bonding which was also confirmed by the crystal structure of compounds **1**. The C=N stretching frequency in all the compounds was observed in the range 1544–1586 cm^{-1} which is intermediate between single and double bond and shows the conjugation between all the three nitrogen atoms of the guanidine moiety [26]. A sharp peak for C=O was also observed in the range 1601–1656 cm^{-1} for all the guanidines.

In the complexes, significant changes were observed in the C=O band which shifted toward smaller value in all complexes showing single bond behavior due to bonding with the metal atom. The disappearance of the weak N–H band was observed, which provides supporting information about the complex formation. The sharp N–H band appeared in the same region with some shift towards higher value. M–O and M–N bands are also observed in the range 443–488 and 272–278 cm^{-1} respectively in all the complexes, which are within the specific regions for Cu–O and Cu–N bond [27].

^{1}H and ^{13}C NMR spectra of all the guanidines were taken in chloroform but the complexes being paramagnetic in nature could not be analyzed by NMR. In ^{1}H NMR compound **2**–**4** have one N–H proton resonating up-field in the range 4.73–4.96 ppm and another one downfield in the range 12.12–12.13 ppm. The downfield proton was identified as the Ph–N*H* proton that appeared downfield due to the attachment of electron withdrawing aromatic groups on nitrogen atoms. The other reason may be the involvement of H–bonding with the carbonyl oxygen. In the remaining compounds (**1** and **5**–**8**) both N–*H* protons appeared downfield in the range 10.30–12.15 ppm due to the presence of aromatic groups on both nitrogen atoms. Moreover the signals of the NH protons are often broad because the ^{14}N–^{1}H coupling is only partly eliminated by the quadrupole relaxation of ^{14}N, due to which –NH–*CH*$_2$– show spin–spin decoupling effect and not couple with each other. The methylene protons appear as a broad singlet (pyramid like) due to "methylene enveloping" and keto-enol tautomerism existing in these guanidine structures, which also justify the broadening of NH proton and the appearance of NH–*CH*$_2$– methylene protons as a broad pyramid like singlet [28]. Aromatic protons were not well resolved and appeared as complex patterns in their specific region. In ^{13}C NMR, the carbonyl carbon appeared at 176.7–178.4 ppm in all compounds, while the CN_3 carbon was present at 156.0–158.7 ppm which is the specific region for the guanidine moiety [29].

All the synthesized complexes were characterized by elemental analysis using a CHNS analyzer and atomic absorption spectroscopy was used to find the concentration of copper. The results indicated that the ligand to metal ratio in complexes is 1:2 which was further confirmed by the crystal structures of complexes **2a** and **4a**.

2.3. Magnetic susceptibility

Magnetic susceptibility of the synthesized complexes was determined by the magnetic susceptibility balance model Auto MSB. All the complexes were paramagnetic with magnetic moments (μ) in the range of 1.60–1.67 BM, which is characteristic for the 3 d^{9} electronic configuration of Cu(II) complexes.

2.4. Structural studies

Compound **1**, Fig. 1, is a typical N,N′,N″-trisubstituted guanidine with normal geometric parameters [30]. In the asymmetric unit, there are two independent molecules with slightly different conformations. The C–O bond distance indicates that the bond has full double bond character while the C–N bond lengths indicate partial double bond character (Table 2). The guanidine moiety and carbonyl group are coplanar due to intramolecular N–H…O hydrogen bonding, forming a six-membered ring commonly observed in this class of compounds (Table 3).

The compounds **2a** and **4a**, are the copper(II) complexes with the anionic bidentate chelating ligands, **2** and **4**, respectively, as shown in Figs. 2 and 3. Each complex has a square-planar geometry in which the metal atom lies at an inversion center. Some selected geometric parameters are listed in Table 2. As shown in Table 2, **2a** and **4a** have very similar geometric parameters. The shorter C1–N1

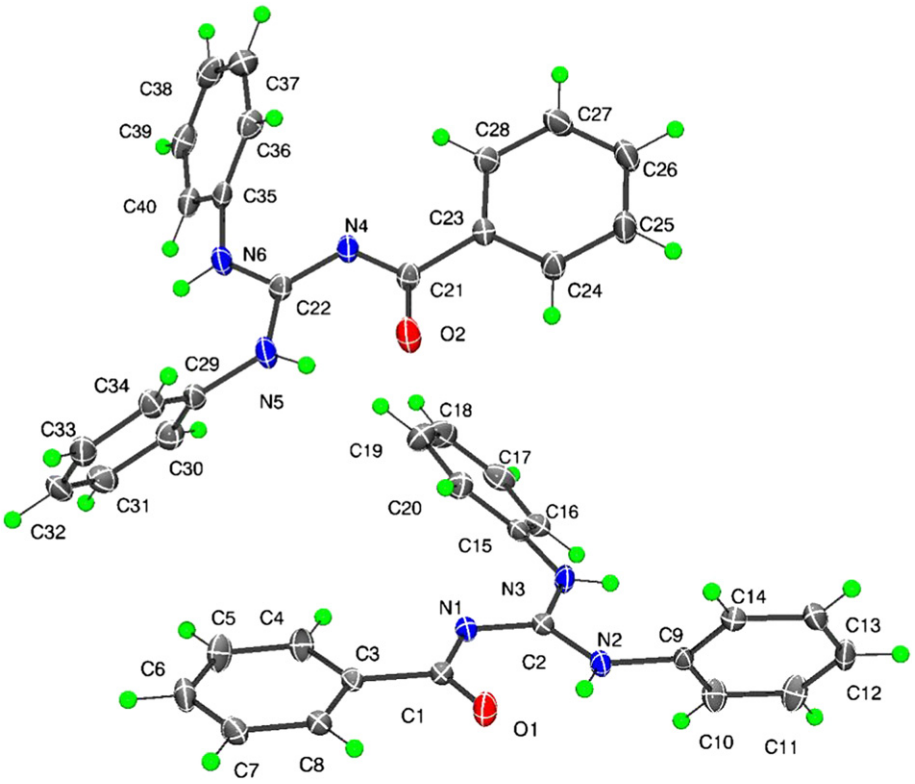

Fig. 1. Molecular diagram of (**1**); displacement ellipsoids are drawn at the 50% probability level.

Table 1
Crystallographic data for **1**, **2a** and **4a**.

	1	**2a**	**4a**
Formula	C_{20} H_{17} N_3 O	C_{36} H_{40} Cu N_6 O_2	C_{40} H_{44} Cu N_6 O_2
FW	315.37	652.28	704.37
Crystal system	Monoclinic	Tetragonal	Monoclinic
Space group	$P2_1/n$	$I\,4_1/a$	$P2_1/n$
a (Å)	13.850(4)	34.330(14)	10.043(3)
b (Å)	13.582(3)		10.584(4)
c (Å)	18.892(5)	5.631(2)	16.180(6)
β(°)	113.890(3)		93.978(4)
V (Å^3)	3249.2(15)	6637(5)	1715.6(10)
Z	8	8	2
T (°C)	−150	−150	−150
D_C Mg/m^3	1.289	1.306	1.363
μ (mm^{-1})	0.082	0.699	0.682
F(000)	1328	2744	742
Crystal size (mm^3)	0.35 × 0.31 × 0.22	0.45 × 0.36 × 0.30	0.30 × 0.25 × 0.20
θ range (°)	3.22 to 27.48	3.36 to 27.47	3.01 to 27.48
Index ranges	−16<=h<=17 −17<=k<=11 −22<=l<=24	−41<=h<=44 −44<=k<=40 −4<=l<=7	−13<=h<=11 −9<=k<=13 −21<=l<=20
Reflections collected	26,248	26,475	14,006
Indept. Reflect. [R(int)]	7416 (0.0325)	3793 (0.0450)	3903 (0.0280)
Completeness to θ = 25.00°	99.5%	99.6%	99.46%
Max. & min. transmission	0.9822 & 0.9720	0.8176 & 0.7437	0.787 & 0.710
Data/restraints/parameters	7416/0/449	3793/0/206	3903/0/231
Goodness-of-fit on F^2	1.15	1.27	1.11
R_1 [$I > 2\sigma(I)$]	0.054	0.052	0.040
wR_2 [all data]	0.111	0.103	0.098
Largest peak and hole (eÅ^{-3})	0.253, −0.190	0.326, −0.434	0.796, −0.479

and longer C1–O1 distance as compared to the corresponding ones in **1** indicate that the C–O has more single bond character and the C–N more double bond character than those in **1**. The plane of the guanidinate moiety (O1/C1/N1/C2/N2/N3) is slightly tilted from the coordination plane of **2**a (CuN_2O_2), 11.02(11)°. It is also observed in the structure of **4a**.

Table 2
Selected bond lengths (Å), angles (°) and torsion angles (°) for **1**, **2a** and **4a**.

1			
O(1)–C(1)	1.247 (17)	O(2)–C(21)	1.247 (18)
N(1)–C(1)	1.359 (18)	N(4)–C(21)	1.359 (18)
N(1)–C(2)	1.339 (17)	N(4)–C(22)	1.334 (18)
N(2)–C(2)	1.338 (18)	N(5)–C(22)	1.344 (19)
N(3)–C(2)	1.357 (18)	N(6)–C(22)	1.355 (19)
O(1)–C(1)–N(1)	127.20(12)	O(2)–C(21)–N(4)	127.36(13)
C(1)–N(1)–C(2)	119.38(12)	C(21)–N(4)-C(22)	118.94(12)
N(1)–C(2)–N(2)	124.28(13)	N(4)–C(22)–N(5)	123.95(13)
N(1)–C(2)–N(3)	118.51(13)	N(4)–C(22)–N(6)	118.94(13)
N(2)–C(2)–N(3)	117.19(12)	N(5)–C(22)–N(6)	117.09(13)
2a			
Cu(1)–O(1)	1.912 (17)	Cu(1)–N(2)	1.966 (18)
O(1)–C(1)	1.277(3)	N(1)–C(1)	1.315(3)
N(1)–C(2)	1.362(3)	N(2)–C(2)	1.339(3)
N(3)–C(2)	1.355(3)		
O(1)–Cu(1)–O(1*)	180.0	N(1)–Cu(1)–N(1*)	180.0
O(1)–Cu(1)–N(1)	90.14(7)	O(1)–Cu(1)–N(1*)	89.86(7)
C(1)–O(1)–Cu(1)	126.20(14)	C(2)–N(1)–Cu(1)	123.69(15)
C(9)–N(2)–Cu(1)	120.26(13)		
4a			
Cu(1)–O(1)	1.909 (14)	Cu(1)–N(2)	1.964 (16)
O(1)–C(1)	1.277(2)	N(1)–C(1)	1.310(2)
N(1)–C(2)	1.363(2)	N(2)–C(2)	1.331(2)
N(3)–C(2)	1.360(2)		
O(1)–Cu(1)–O(1*)	180.0	N(1)–Cu(1)–N(1*)	180.0
O(1)–Cu(1)–N(1)	90.32(6)	O(1)–Cu(1)–N(1*)	89.68(6)
C(1)–O(1)–Cu(1)	126.17(12)	C(2)–N(2)–Cu(1)	124.01(12)
C(9)–N(2)–Cu(1)	120.11(12)		

Table 3
The intramolecular hydrogen bonds for **1**, distance, Å; angle, °.

Compound	D	H	A	DH(Å)	HA(Å)	DA(Å)	DHA(°)
1	N2	H2N	O1	0.870(2)	1.877(19)	2.581 (16)	136.7(17)
	N5	H6N	O2	0.880(2)	1.820(2)	2.551 (17)	139.2(18)

2.5. UV–visible spectroscopy

Fig. 4(a) and 4(b) present the overlay of UV–visible spectra of **3a,** taken in DMSO at different intervals of time *i.e.* for fresh solution (day one), after three, five and seven days. The spectra were recorded for two wavelength ranges with different concentrations, 264–400 nm (1.6×10^{-5} M) and 400–800 nm (1.6×10^{-4} M). The absorption spectra of complex **3a** exhibit bands in the regions 270–280, 290–295(weak shoulder), 525–710 (broad-band) and 735–750 nm. In UV-region, one peak appears at 275 nm, that may be attributed to the $\pi-\pi^*$ transition of benzene rings of the ligands. The appearance of the broad peaks in the 525–710 nm regions corresponds to the *d–d* electronic transition of the metal *d*-orbitals. In DMSO solution, a unique weak absorption at 745 nm is observed [31]. Keeping in view all this, it is perquisite that the copper(II) complexes (**1a**–**8a**) are also stable in test solution medium as well as in solid state.

2.6. Pharmacology

2.6.1. Brine shrimps lethality assay

The cytotoxicity of the synthesized compounds was evaluated by the brine shrimp lethality method as reported earlier [32]. LD_{50} was calculated which showed that most of the compounds had good cytotoxic activities. Compound **2** is the most active of all the compounds with LD_{50} 1.7 μg/ml, while the rest of the compounds showed activities with LD_{50} ranging from 20 to 779 μg/ml. Results, given in Table 4, indicate that the guanidines (**1**–**8**) show good cytotoxic activities; similar results were observed with the copper complexes (**1a**–**8a**). The active compounds showed concentration-dependent toxicities, as reported earlier [33].

2.6.2. In vitro cytotoxicity screening

As brine shrimps assay (a prescreening test for antitumor activities) showed good results, these compounds were further evaluated for their *in vitro* cytotoxicity in human cell lines.

Thus far little is known in a systematic way about the *in vitro* cytotoxicity of copper complexes. Mostly some compounds have been studied, large series of compounds have not been tested [15–17,34–36]. It has been suggested that copper complexes may function as a topoisomerase II inhibitor [17], anyhow DNA binding has been mentioned [36]. In the present series of copper complexes of guanidines ID_{50} values were in the high range of those of cisplatin. Aryl substituted compounds are the most active, in particular C_6H_5 substituted. There is no consistent similar trend in activity as to the different cell lines. This indicates that there is room for structural variation affecting different cell lines in a different way. When extrapolated to the human clinical situation this observation might be of importance. It is not yet clear which factors, such as size or electronic properties of the substituent are relevant to the *in vitro* cytotoxic activity. ID_{50} values in Table 7 indicate that **1a** is more active than the standard drug etoposide (ETO) against lungs carcinoma cells (H226), whereas, **7a** have shown a comparable activity against the same. In short, data collected so far indicate promising *in vitro* cytotoxicity. They constitute a highly useful reference basis for future further investigations.

2.6.3. In vitro antibacterial activity

Antibacterial screening of the synthesized compounds was carried out by using four bacterial strains two Gram positive *Staphylococcus aureus* (ATCC 6538), *Micrococcus luteus* (ATCC 10240) and two Gram negative, *Escherichia coli* (ATCC 15224), *Salmonella setubal* (ATCC 19196). The zones of inhibition values in Table 5 represent the mean value of the three readings with standard deviation [STDEV]. Zones of more than 12 mm are characteristic for significant activities, 10–12 mm, for good activities, 7–9 mm low, and below 7 mm, non-significant activities.

The results revealed that compound **2** show**s** good to low activity against *M. luteus*, *S. setubal* and *S. aureus* and that compound **7a** shows some activity against *M. luteus* and *S. aureus*.

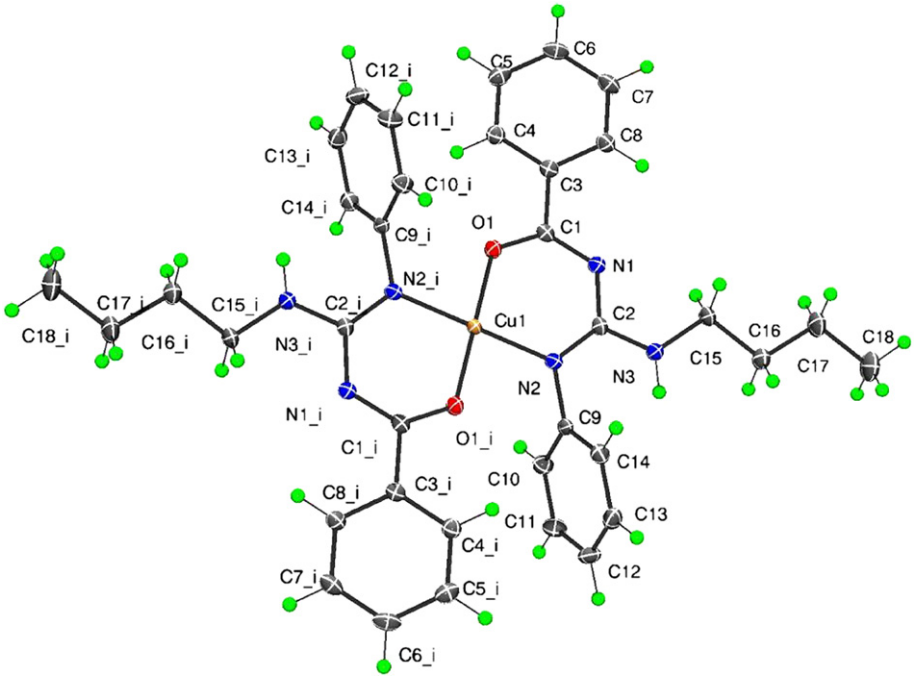

Fig. 2. Molecular diagram of (**2a**); displacement ellipsoids are drawn at the 50% probability level.

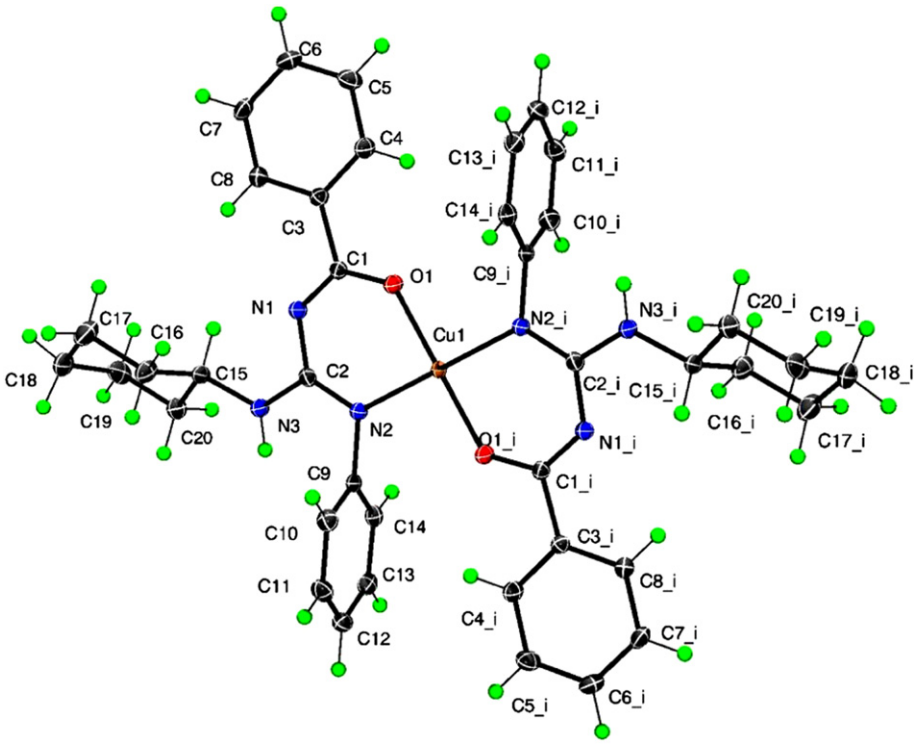

Fig. 3. Molecular diagram of (**4a**); displacement ellipsoids are drawn at the 50% probability level.

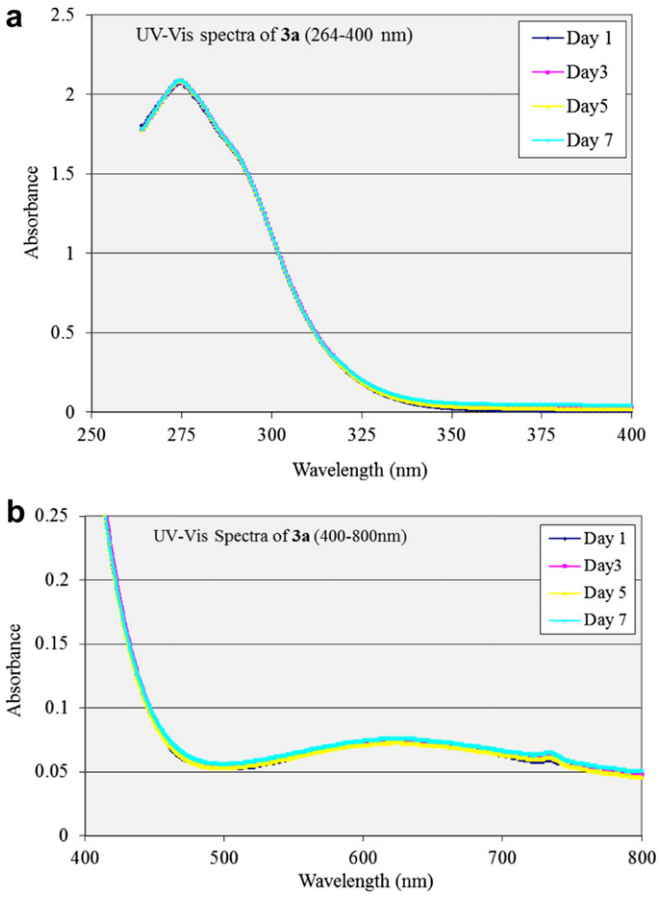

Fig. 4. (a) UV–visible spectra of **3a** (264–400 nm, 1.6×10^{-5} M), taken in DMSO for fresh solution (day one), after three, five and seven days. (b) UV–visible spectra of **3a** (400–800 nm, 1.6×10^{-4} M), taken in DMSO for fresh solution (day one), after three, five and seven days.

None of the compounds showed activity against *E. coli*. Previously the activity was shown by the guanidine ligands to some extent [37,38], while Cu enhanced the antibacterial activity of the guanidine ligands [39].

2.6.4. Antifungal activity

All the synthesized compounds were subjected to antifungal assays by using the Agar tube dilution method [40] against four fungal strains i.e. *Mucor species, Aspergillus niger, Aspergillu flavus,* and *Fusarium solani*. The terbinafine was used as standard drug and the results are summarized in the Table 6. The activity was investigated on the basis of percent growth inhibition; inhibition more than 70% was considered a significant activity, 60–70% good, 50–60% moderate and below 50% non-significant.

The complex **5a** showed good activity against *Mucor, A. niger,* and *F. solani* while compound **7, 8** and **1a** showed good activities

Table 4
Brine shrimps assay for guanidine ligands (**1, 2, 5–8**) and complexes (**1a–3a, 5a–8a**).

Test compounds	Percentage mortality of brine shrimps at concentrations			LD_{50} (μg/ml)
	1000 ppm	100 ppm	10 ppm	
1	80	10	0	301.73
2	100	100	100	1.701
5	40	14	0	360.38
6	100	40	0	96.03
7	100	80	25	20.30
8	100	30	0	149.72
1a	67	40	20	310.22
2a	65	15	0	535.35
3a	70	50	5	111.82
5a	57	10	0	779.44
6a	100	20	7	146.74
7a	100	47	17	70.74
8a	100	20	0	183.28

Table 5
In vitro antibacterial activity of synthesized guanidines (**1, 2, 5**–**8**), complexes (**1a**–**3a, 5a**–**8a**) and standard drugs.

Test compounds	% zone of inhibition of samples (mm)			
	M. luteus	*E. coli*	*S. setubal*	*S. aureus*
1	–	–	–	–
2	10.8 ± 0.163 1 mg/ml	–	7.4 ± 0.081 1 mg/ml	12.5 ± 0.81 0.4 mg/ml
5	–	–	–	–
6	–	–	–	–
7	–	–	–	–
8	–	–	–	–
1a	–	–	–	–
2a	–	–	–	–
3a	–	–	–	–
5a	–	–	–	–
6a	–	–	–	–
7a	11 ± 0.408 0.8 mg/ml	–	–	12 ± 0.20 0.6 mg/ml
8a	–	–	–	7.7 ± 0.20 1 mg/ml
Roxithromycin	36 ± 0.577	30.3 ± 1.02	19.7 ± 0.88	37 ± 0.57
Cefixime	46.33 ± 0.33	56 ± 2.30	44.6 ± 0.70	49.3 ± 0.33
DMSO	–	–	–	–

± - mean standard deviation of triplicate, (–)- no zone of inhibition observed, Roxithromycin and Cefixime -as positive control, DMSO-as negative control.

against *F. solani* and compound **1** against the *Mucor species*. The rest of the compounds did not show significant activities. The overall results show that guanidine ligands had good/moderate antifungal activities with little enhancement when these guanidine were coordinated with copper. According to some previous studies guanidines have shown similar results [15,41].

3. Conclusion

In the present study of guanidine ligands and their complexes it has been shown that guanidine ligands exhibit anti-microbial and cytotoxic activities and that almost similar results are shown by their Cu complexes with a little enhancement. The cytotoxicity data obtained show an interesting variable pattern among the different human cell lines. They constitute a valuable starting point for future investigations. ID_{50} values indicate that **1a** and **7a** have shown promising results against lungs carcinoma cells (H226). UV–Visible studies in DMSO solutions indicate that the copper(II) complexes (**1a**–**8a**) are also stable in in test solution medium as well.

Table 6
Antifungal activity of guanidine ligands (**1, 2, 5**–**8**) and complexes (**1a**–**3a, 5a**–**8a**).

Test compounds	Compounds showing %inhibition against fungal strains			
	A. Niger	*F. Solani*	*Mucor*	*A. Flavus*
1	43.90	42.36	64.28	41.8
2	–4.87	51.3	39.28	34.6
5	37.19	55.5	61.30	–2.0
6	36.58	9.72	44.04	18.3
7	24.39	63.88	35.11	36.7
8	40.24	64.58	41.07	16.3
1a	–2.43	61.8	–4.16	39.7
2a	0	75	40.47	–3.0
3a	26.8	62.5	20.83	16
5a	62.19	52.7	76.19	36
6a	52.43	54.1	–4.16	35
7a	9.75	53.5	1.78	46.8
8a	30.48	54.8	43.45	62.2
Terbinafine	100	100	100	100
Linear length in -ve control	41	72	84	49

4. Experimental

4.1. Materials and methods

All experiments were carried out under the specified conditions of temperature. Solvents were distilled from the drying agents and degassed before use.

NMR spectra were recorded on a Bruker ARX, 300 MHz spectrometer. ^{1}H NMR (300.13 MHz): internal standard solvent $CDCl_3$ (7.28 ppm from TMS): internal standard TMS; ^{13}C NMR (75.47 MHz): internal standard solvent $CDCl_3$ (77.0 ppm from TMS): internal standard TMS; the splitting of proton resonances in the reported ^{1}H NMR spectra are defined as s = singlet, d = doublet, t = triplet, q = quartet and m = complex pattern; coupling constants are reported in Hz. FT–IR spectra were recorded as KBr pellets on a Bio-Rad Excalibur FT–IR Model FTS 3000 MX (400–4000 cm^{-1}) and on ATR with Perkin Elmer System 2000 (200–500 cm^{-1}). The elemental analyses were performed using a LECO-932 CHNS analyzer while the metal concentrations were determined on an Atomic Absorption Spectrophotometer Perkin Elmer 2380. Magnetic susceptibilities of the complexes (**1a**–**8a**) were recorded with a Magnetic Susceptibility Balance Auto MSB. Absorption spectra were measured on a UV–Visible spectrometer; Shimadzu 1800 at constant temperature of 25 ± 1 °C. The melting points were determined on a Bio Cote SMP10- UK and are uncorrected. All solvents were purified by distillation, dried under an atmosphere of nitrogen and stored over molecular sieves 4 Å.

Benzoic acid, potassium thiocyanate, thionyl chloride, aniline, triethylamine, mercuric chloride, *n*-butylamine, *sec*-butylamine, cyclohexylamine, 1-naphthylamine, 2,4-dichloroaniline, 3,4-dichloroaniline, 3,5-dichloroaniline and copper(II) acetate were purchased from Sigma–Aldrich and used as received without further purification.

4.2. Synthesis of N,N′,N″-trisubstituted guanidine ligands (*1*–*8*)

The guanidine ligands were synthesized from N-benzoyl-N′-phenylthiourea, by using a standard guanylation reaction method [25a]. N-benzoyl-N′-phenylthiourea was mixed in a 1:1 M ratio with the desired substituted aniline in DMF in which triethylamine was already added in 2 M ratio. The reaction mixture was maintained at temperatures below 5 °C by applying an ice bath. Mercuric chloride (1:1) was added to the reaction mixture and vigorously stirred for overnight. Progress of reaction was monitored by TLC until all the thiourea was consumed. Chloroform (20 ml) was added and the suspension was filtered through a sintered glass funnel to remove the residue (HgS). The solvents were evaporated under reduced pressure and the residue was dissolved in 20 ml of CH_2Cl_2, washed with water (4 × 30 ml) and the organic phase was dried over anhydrous $MgSO_4$. The solvent was evaporated and the residue was recrystallized from ethanol to get the crystals of the compounds (**1**–**8**) (see Scheme 1)

4.2.1. N,N′-diphenyl-N″-benzoylguanidine (*1*)

Quantities used were 5.6 ml (40 mmol) triethylamine, 2.0 ml (20 mmol) aniline 5.12 g (20 mmol) of N-benzoyl-N′-phenylthiourea and 5.44 g (20 mmol) mercuric chloride; Yield 4.54 g, 72%; yellowish white solid; m.p. 96–98 °C; FT–IR (KBr, cm^{-1}) 3389, 3157, 3054, 1603, 1562, 1526, 1491, 1446, 1351, 1022, 901, 750, 693, 511, 480; ^{1}H NMR (300 MHz, $CDCl_3$, 25 °C) δ 7.29–7.80 (m, 13H, Ar*H*), 8.25 (d, 2H, J = 7.2 Hz, Ar$H_{c=c'}$), 10.30 (br, s, 2H, R–N*H*); ^{13}C NMR (75.47 MHz, $CDCl_3$, 25 °C) δ 124.3 (4C), 126.1 (2C), 128.0 (2C), 129.3 (2C), 129.5 (4C), 131.5, 136.4, 138.1 (2C) (Aromatic–*C*), 156.6 (*C*, CN_3), 178.3 (*C*, C=O); Anal. Calcd. for $C_{20}N_3H_{17}O$ (315.37): C, 76.17; H, 5.43; N, 13.32; Found: C, 76.23; H, 5.67; N, 13.40.

Table 7
Cytotoxicity of some selected copper(II) complexes of guanidines**1a**, **2a**, **3a**, **5a**, **7a**, and **8a**, and of some reference compounds like doxorubicin (DOX), cisplatin (CPT), 5-flourouracil (5-FU), methotrexate (MTX), etoposide (ETO) and taxol (TAX). ID_{50} values (ng/ml) of test compounds *in vitro* using SRB as cell viability test.

Test compounds	Human cell line						
	A498 (Renal-F)	EVSA-T (Breast)	H226 (Lungs)	IGROV (Ovarian)	M19MEL (Melanoma -Skin)	MCF-7 (Breast)	WIDR (Colon)
1a	4254	7578	2998	2955	1959	7765	8359
2a	41062	12002	18845	29840	4779	15593	7048
3a	25000	10870	16617	27083	3428	16971	11152
5a	23911	6365	12854	24709	2901	8544	14672
7a	10454	3334	7046	8480	1196	6080	8394
8a	22351	7507	13190	24133	2413	9893	10786
DOX	90	8	199	60	16	10	11
CPT	2253	422	3269	169	558	699	967
5-FU	143	475	340	297	442	750	225
MTX	37	5	2287	7	23	18	< 3.2
ETO	1314	317	3934	580	505	2594	150
TAX	<3.2	<3.2	<3.2	<3.2	< 3.2	<3.2	<3.2

In separate experiments an inter-experimental CV of 1–11% and an intra-experimental CV of 2–4% were obtained.

*4.2.2. N-phenyl-N′-(n-butyl)-N″-benzoylguanidine (**2**)*

Quantities used were 5.6 ml (40 mmol) triethylamine, 2.0 ml (20 mmol) *n*-butylamine, 5.12 g (20 mmol) N-benzoyl-N′-phenyl-thiourea and 5.44 g (20 mmol) mercuric chloride. Yield 4.96 g, 84%; yellowish white solid; m.p. 88–90 °C; FT–IR (KBr, cm^{-1}) 3288, 3062, 2959, 2926, 2866, 1620, 1544, 1500, 1495, 1394, 1352, 1256, 1144, 1069, 1023, 907, 812, 752, 698, 617, 565, 499; ^{1}H NMR (300 MHz, $CDCl_3$, 25 °C) δ 0.97 (t, 3H, J = 7.2 Hz, CH_3–CH_2–CH_2–CH_2–), 1.40 (tq, 2H, J = 7.2, 7.5 Hz, CH_3–CH_2–CH_2–CH_2–), 1.61 (tt, 2H, J = 7.2, 7.5 Hz, CH_3–CH_2–CH_2–CH_2–) 3.55 (br, s, 2H, NH–CH_2–CH_2–), 4.96 (br, s, 1H, R–N*H*), 7.28–7.49 (m, 8H, Ar*H*), 8.29 (d, 2H, J = 6.9 Hz, Ar$H_{c=c'}$), 12.12 (br, s, 1H, Ph–N*H*); ^{13}C NMR (75.47 MHz, $CDCl_3$, 25 °C) δ 13.8 (CH_3), 20.1 (CH_3–CH_2), 31.8 (CH_2–CH_2–CH_2), 41.2 (NH–CH_2), 125.5 (2C), 126.8, 127.9 (2C), 129.1 (2C), 130.0 (2C), 131.2, 136.2, 138.6 (Aromatic–*C*), 158.7 (*C*, CN_3), 177.5 (*C*, C=O); Anal. Calcd. for $C_{18}N_3H_{21}O$ (295.38): C, 73.19; H, 7.17; N, 14.23; Found: C, 73.23; H, 7.23; N, 14.31.

*4.2.3. N-phenyl-N′-(sec-butyl)-N″-benzoylguanidine (**3**)*

Quantities used were 5.6 ml (40 mmol) triethylamine, 2.1 ml (20 mmol) *sec*-butylamine, 5.12 g (20 mmol) N-benzoyl-N′-phenyl-thiourea and 5.44 g (20 mmol) mercuric chloride; Yield 4.67 g, 79%; yellowish white solid; m.p. 61–63 °C; FT–IR (KBr, cm^{-1}) 3246, 2963, 2930, 2872, 1656, 1576, 1496, 1377, 1225, 1135, 1067, 1020, 894, 746, 716, 679, 589, 490; ^{1}H NMR (300 MHz, $CDCl_3$, 25 °C) δ 0.98 (t, 3H, J = 7.2 Hz, terminal CH_3), 1.23 (d, 3H J = 6.6 Hz, branched CH_3), 1.57 (tt, 2H, J = 7.2, 7.2 Hz, CH_2), 4.37 (br, s, 1H, C*H*), 4.73 (br, s, 1H, R–N*H*), 7.17–7.92 (m, 8H, Ar*H*), 8.29 (d, 2H, J = 6.9 Hz, Ar$H_{c=c'}$), 12.13 (br, s, 1H, Ph–N*H*); ^{13}C NMR (75.47 MHz, $CDCl_3$, 25 °C) δ 10.5 terminal CH_3), 20.6 (branched CH_3), 29.6 (CH_2), 48.7 (*C*H), 125.4 (2C), 126.7, 127.9 (2C), 129.1 (2C), 130.1 (2C), 131.2, 136.2, 138.8 (Aromatic–*C*), 158.2 (*C*,CN_3), 177.5 (*C*, C=O); Anal. Calcd. for $C_{18}N_3H_{21}O$ (295.38): C, 73.19; H, 7.17; N, 14.23; Found: C, 73.30; H, 7.05; N, 14.43.

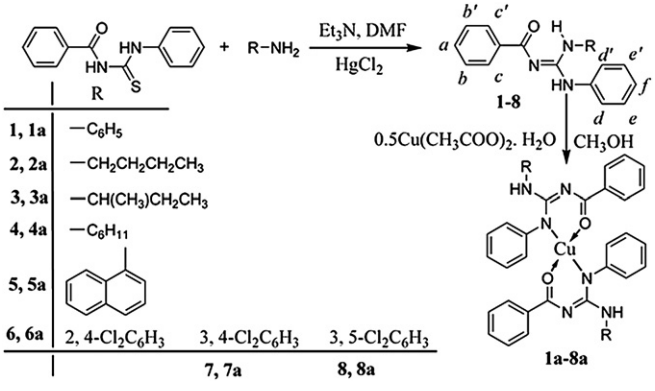

Scheme 1. Synthesis of N,N′,N″-trisubstituted guanidines (**1**–**8**) and their copper(II) complexes (**1a**–**8a**).

*4.2.4. N-phenyl-N′-cyclohexyl-N″-benzoylguanidine (**4**)*

Quantities used were 5.6 ml (40 mmol) triethylamine, 2.3 ml (20 mmol) cyclohexylamine, 5.12 g (20 mmol) N-benzoyl-N′-phenylthiourea and 5.44 g (20 mmol) mercuric chloride; Yield 5.27 g, 82%; colourless solid; m.p. 120–123 °C; FT–IR (KBr, cm^{-1}) 3326, 3235, 3060, 2930, 2853, 1623, 1586, 1564, 1496, 1448, 1254, 1142, 1026, 901, 837, 760, 691, 580, 493; ^{1}H NMR (300 MHz, $CDCl_3$, 25 °C) δ 1.23–2.09 (m, 11H, cyclohexyl–*H*), 4.86 (br, s, 1H, R–N*H*) 7.28–7.49 (m, 10H, Ar*H*), 8.25 (d, 2H, J = 7.2 Hz, Ar$H_{c=c'}$), 12.12 (br, s, 1H, Ph–N*H*); ^{13}C NMR (75.47 MHz, $CDCl_3$, 25 °C) δ 24.8 (*C*–3 and *C*–5 in cyclohexyl), 25.6 (*C*–4 in cyclohexyl), 33.1 (*C*–2 and *C*–6 in cyclohexyl), 50.2 (*C*–1 in cyclohexyl), 125.2 (2C), 126.6, 127.9 (2C), 129.1 (2C), 130.0 (2C), 131.5, 136.3, 138.7 (Aromatic–*C*), 157.8 (*C*, CN_3), 177.5 (*C*, C=O); Anal. Calcd. for $C_{20}N_3H_{23}O$ (321.4): C, 74.70; H, 7.21; N, 13.07; Found: C, 74.34; H, 7.40; N, 12.96.

*4.2.5. N-phenyl-N′-(1-naphthyl)-N″-benzoylguanidine (**5**)*

Quantities used were, 5.6 ml (40 mmol) triethylamine, 2.86 g (20 mmol) 1-naphthylamine, 5.12 g (20 mmol) N-benzoyl-N′-phenylthiourea and 5.44 g (20 mmol) mercuric chloride; Yield 5.48 g, 75%; light brown solid; m.p. 132–134 °C; FT–IR (KBr, cm^{-1}) 3351, 3052, 1614, 1561, 1449, 1352, 1240, 777, 751, 692, 616; ^{1}H NMR (300 MHz, $CDCl_3$, 25 °C) δ 7.18–8.17 (m, 15H, Ar*H*), 8.31 (d, 2H, J = 6.0 Hz, Ar$H_{c=c'}$), 10.54 (br, s, 1H, R–N*H*), 12.15 (br, s, 1H, Ph–N*H*); ^{13}C NMR (75.47 MHz, $CDCl_3$, 25 °C) δ 120.1, 122.5, 123.4, 124.2, 125.2 (2C), 125.8, 127.1, 127.5, 128.1 (2C), 128.6, 129.0 (2C), 129.4 (2C), 131.5, 131.9, 134.7, 137.1, 138.3 (Aromatic–*C*), 157.7 (*C*, CN_3), 178.6 (*C*, C=O); Anal. Calcd. for $C_{24}N_3H_{19}O$ (365.43): C, 78.88; H, 5.24; N, 11.50; Found: C, 78.57; H, 4.93; N, 11.75.

*4.2.6. N-phenyl-N′-(2,4-dichlorophenyl)-N″-benzoylguanidine (**6**)*

Quantities used were 5.6 ml (40 mmol) triethylamine, 3.3 g (20 mmol) 2,4-dichloroaniline, 5.12 g (20 mmol) N-benzoyl-N′-phenylthiourea and 5.44 g (20 mmol) mercuric chloride; Yield 5.84 g, 76%; colourless solid; m.p. 156–158 °C; FT–IR (KBr, cm^{-1}) 3379, 3166, 3058, 1601, 1561, 1519, 1362, 1292, 1192, 811, 745, 699, 588, 487; ^{1}H NMR (300 MHz, $CDCl_3$, 25 °C) δ 7.04–8.40 (m, 11H, Ar*H*), 8.21 (d, 2H, J = 9.0 Hz, Ar$H_{c=c'}$), 10.88 (br, s, 1H, R–N*H*), 12.13 (br, s, 1H, Ph–N*H*); ^{13}C NMR (75.47 MHz, $CDCl_3$, 25 °C) δ 122.3, 123.9, 125.6, 125.8 (2C), 127.1, 127.4, 127.6 (2C), 128.9, 129.2 (2C), 130.1 (2C), 131.8, 135.2, 137.8, 140.7 (Aromatic–*C*), 156.0 (*C*, CN_3), 178.5 (*C*, C=O); Anal. Calcd. for $C_{20}N_3H_{15}OCl_2$ (384.26): C, 62.51; H, 3.93; N, 10.94; Found: C, 62.43; H, 3.71; N, 10.99.

*4.2.7. N-phenyl-N′-(3,4-dichlorophenyl)-N″-benzoylguanidine (**7**)*

Quantities used were 5.6 ml (40 mmol) triethylamine, 3.3 g (20 mmol) 3,4-dichloroaniline, 5.12 g (20 mmol) N-benzoyl-N′-phenylthiourea and 5.44 g (20 mmol) mercuric chloride; Yield 5.69 g, 74%; yellow solid; m.p. 99–100 °C; FT–IR (KBr, cm^{-1}) 3393, 3162, 3062, 1603, 1561, 1516, 1356, 1281, 1194, 1129, 1024, 905, 745, 695, 588, 490; ^{1}H NMR (300 MHz, $CDCl_3$, 25 °C) δ 7.13–8.24 (m, 11H, Ar*H*), 8.36 (d, 2H, J = 8.1 Hz, Ar$H_{c=c'}$), 10.53 (br, s, 1H, R–N*H*), 11.98 (br, s, 1H, Ph–N*H*); ^{13}C NMR (75.47 MHz, $CDCl_3$, 25 °C) δ 121.5, 125.5 (2C), 127.0, 127.4, 128.2 (2C), 129.3 (2C), 130.2 (2C), 130.4, 131.8, 132.7, 133.4, 135.8, 136.6, 137.3 (Aromatic–*C*), 156.1 (*C*, CN_3), 178.4 (*C*, C=O); Anal. Calcd. for $C_{20}N_3H_{15}OCl_2$ (384.26): C, 62.51; H, 3.93; N, 10.94; Found: C, 62.26; H, 3.91; N, 10.98.

*4.2.8. N-phenyl-N′-(3,5-dichlorophenyl)-N″-benzoylguanidine (**8**)*

Quantities used were 5.6 ml (40 mmol) triethylamine, 3.3 g (20 mmol) 3,5-dichloroaniline, 5.12 g (20 mmol) N-benzoyl-N′-phenylthiourea and 5.44 g (20 mmol) mercuric chloride; Yield 5.53 g, 72%; yellow solid; m.p. 112–114 °C; FT–IR (KBr, cm^{-1}) 3382, 3194, 3056, 1609, 1565, 1508, 1369, 1258, 1114, 908, 803, 757, 687, 582, 490; ^{1}H NMR (300 MHz, $CDCl_3$, 25 °C) δ 7.06–7.78 (m, 11H, Ar*H*), 8.24 (d, 2H, J = 7.5 Hz, Ar$H_{c=c'}$), 10.51 (br, s, 1H, R–N*H*), 12.02 (br, s, 1H, Ph–N*H*); ^{13}C NMR (75.47 MHz, $CDCl_3$, 25 °C) δ 124.3 (2C), 126.3 (2C), 126.7 (2C), 127.1, 129.0 (2C), 129.4, 130.2 (2C), 130.6, 133.9 (2C), 134.3, 137.4, 137.8 (Aromatic–*C*), 157.3 (*C*, CN_3), 176.7 (*C*, C=O); Anal. Calcd. for $C_{20}N_3H_{15}OCl_2$ (384.26): C, 62.51; H, 3.93; N, 10.94; Found: C, 62.32; H, 4.06; N, 11.05.

*4.3. Synthesis of complexes (**1a**–**8a**)*

The solution of $Cu(CH_3COO)_2.H_2O$ (1 mmol) in dry methanol (20 ml) was added into the solution of an appropriate guanidine (2 mmol) in methanol (15 ml) at room temperature [25b]. The reaction mixture was stirred for 4 h under an inert atmosphere; then the precipitates were filtered and washed with methanol (Scheme 1). These precipitates were dissolved in a $CHCl_3$/*n*-hexane mixture (1:1) and kept for slow evaporation to give the crystals of the desired complexes which were isolated mechanically from the mother liquor.

*4.3.1. Bis(N,N′-diphenyl-N″-benzoylguanidinato)copper(II) (**1a**)*

Quantities used were 1.26 g (4 mmol) N,N′-diphenyl-N"-benzoylguanidine (**1**) and 0.4 g (2 mmol) $Cu(CH_3COO)_2.H_2O$; Yield 1.11 g, 80%; blue solid; m.p. 226–228 °C (decompose); FT–IR (KBr, cm^{-1}) 3404, 3059, 1591, 1557, 1516, 1420, 1369, 1217, 1069, 745, 695, 555, 480, 429, 274; Anal. Calcd. for $C_{40}N_6H_{32}O_2Cu$ (692.27): C, 69.40; H, 4.66; N, 12.15; Cu, 9.18; Found: C, 69.75; H, 4.54; N, 12.48; Cu, 8.86; μ_{eff}, 1.64 BM.

*4.3.2. Bis(N-phenyl-N′-(n-butyl)-N″-benzoylguanidinato)copper(II) (**2a**)*

Quantities used were 1.18 g (4 mmol) N-phenyl-N′-(*n*-butyl)-N″-benzoylguanidine (**2**) and 0.4 g (2 mmol) $Cu(CH_3COO)_2.H_2O$; Yield 1.13 g, 87%; blue solid; m.p. 203–205 °C; FT–IR (KBr, cm^{-1}) 3426, 3055, 2953, 2904, 2867, 1592, 1560, 1518, 1440, 1373, 753, 709, 527, 480, 444, 273; Anal. Calcd. for $C_{36}N_6H_{40}O_2Cu$ (652.29): C, 66.29; H, 6.18; N, 12.88; Cu, 9.74; Found: C, 65.97; H, 5.99; N, 13.05; Cu, 9.20; μ_{eff}, 1.61 BM.

*4.3.3. Bis(N-phenyl-N′-(sec-butyl)-N″-benzoylguanidinato) copper(II) (**3a**)*

Quantities used were 1.18 g (4 mmol) N-phenyl-N′-(*sec*-butyl)-N″-benzoylguanidine (**3**) and 0.4 g (2 mmol) $Cu(CH_3COO)_2.H_2O$; Yield 1.06 g, 81%; blue solid; m.p. 192–194 °C; FT–IR (KBr, cm^{-1}) 3420, 3053, 2963, 2930, 2874, 1592, 1561, 1524, 1447, 1377, 750, 704, 583, 488, 450, 275; Anal. Calcd. for $C_{36}N_6H_{40}O_2Cu$ (652.29): C, 66.29; H, 6.18; N, 12.88; Cu, 9.74; Found: C, 66.15; H, 6.16; N, 12.98; Cu, 9.43; μ_{eff}, 1.62 BM.

*4.3.4. Bis(N-phenyl-N′-cyclohexyl-N″-benzoylguanidinato) copper(II) (**4a**)*

Quantities used were 1.28 g (4 mmol) N-phenyl-N′-cyclohexyl-N"-benzoylguanidine (**4**) and 0.4 g (2 mmol) $Cu(CH_3COO)_2.H_2O$; Yield 1.1 g, 78%; blue solid; m.p. 225–226 °C; FT–IR (KBr, cm^{-1}) 3410, 3052, 2922, 2849, 1590, 1548, 1521, 1447, 1434, 1372, 750, 700, 565, 509, 438, 274; Anal. Calcd. for $C_{40}N_6H_{44}O_2Cu$ (704.36): C, 68.21; H, 6.33; N, 11.93; Cu, 9.02; Found: C, 67.93; H, 6.12; N, 12.10; Cu, 8.89; μ_{eff}, 1.62 BM.

*4.3.5. Bis(N-phenyl-N′-(1-naphthyl)-N″-benzoylguanidinato) copper(II) (**5a**)*

Quantities used were 1.46 g (4 mmol) N-phenyl-N′-(1-naphthyl)-N″-benzoylguanidine (**5**) and 0.4 g (2 mmol) $Cu(CH_3COO)_2.H_2O$; Yield 76%; dirty greenish solid; m.p. 204–205 °C; FT–IR (KBr, cm^{-1}) 3397, 3053, 1589, 1542, 1518, 1424, 1372, 781, 746, 704, 578, 484, 419, 276; Anal. Calcd. for $C_{48}N_6H_{36}O_2Cu$ (792.38): C, 72.76; H, 4.58; N, 10.61; Cu, 8.02; Found: C, 72.46; H, 4.48, N, 10.82; Cu, 7.58; μ_{eff}, 1.60 BM.

*4.3.6. Bis(N-phenyl-N′-(2,4-dichlorophenyl)-N″-benzoylguanidinato) copper(II) (**6a**)*

Quantities used were 1.54 g (4 mmol) N-phenyl-N′-(2,4-dichlorophenyl)-N″-benzoylguanidine (**6**) and 0.4 g (2 mmol) $Cu(CH_3COO)_2.H_2O$; Yield 80%; blue solid; m.p. 222–224 °C; FT–IR (KBr, cm^{-1}) 3381, 3056, 1591, 1546, 1519, 1434, 1369, 745, 698, 612, 584, 509, 485, 443, 273; Anal. Calcd. for $C_{40}N_6H_{28}O_2Cl_4Cu$ (830.05): C, 57.88; H, 3.40; N, 10.12; Cu, 7.66; Found: C, 57.39; H, 3.31; N, 10.17; Cu, 7.35; μ_{eff}, 1.67 BM.

*4.3.7. Bis(N-phenyl-N′-(3,4-dichlorophenyl)-N″-benzoylguanidinato) copper(II) (**7a**)*

Quantities used were 1.54 g (4 mmol) N-phenyl-N′-(3,4-dichlorophenyl)-N″-benzoylguanidine (**7**) and 0.4 g (2 mmol) $Cu(CH_3COO)_2.H_2O$; Yield 76%; blue solid; m.p. 213–214 °C; FT-IR (KBr, cm^{-1}) 3399, 3056, 1586, 1550, 1516, 1438, 1370, 745, 699, 610, 584, 500, 479, 439, 275; Anal. Calcd. for $C_{40}N_6H_{28}O_2Cl_4Cu$ (830.05): C, 57.88; H, 3.40; N, 10.12; Cu, 7.66; Found: C, 57.38; H, 3.39; N, 10.24; Cu, 7.56; μ_{eff}, 1.66 BM.

*4.3.8. Bis(N-phenyl-N′-(3,5-dichlorophenyl)-N″-benzoylguanidinato) copper(II) (**8a**)*

Quantities used were 1.54 g (4 mmol) N-phenyl-N′-(3,5-dichlorophenyl)-N″-benzoylguanidine (**8**) and 0.4 g (2 mmol) $Cu(CH_3COO)_2.H_2O$; Yield 83%; blue solid; m.p. 218–220 °C; FT-IR (KBr, cm^{-1}) 3391, 3061, 1586, 1554, 1518, 1460, 1437, 1364, 745, 696, 669, 566, 502, 465, 430, 274; Anal. Calcd. for $C_{40}N_6H_{28}O_2Cl_4Cu$ (830.05): C, 57.88; H, 3.40; N, 10.12; Cu, 7.66; Found: C, 57.55; H, 3.07; N, 9.84; Cu, 7.27; μ_{eff}, 1.65 BM.

*4.4. Data collection and structural refinement of **1**, **2a** and **4a***

Crystals of the guanidine **1** and complexes **2a** and **4a** were grown by the slow evaporation method. The solvent systems for crystal growth were ethanol for the guanidines and petroleum-ether/chloroform (1:1) for the complexes. The yellowish guanidine and blue complex crystals were mounted in a random orientation on a glass fiber and the reflection data were collected on a Rigaku AFC7R Mercury CCD diffractometer with a graphite monochromated MoKα radiation (λ = 0.71073Å). The structures were solved by using direct methods Sir 97 [42] and refined with Shelxl 97 [43]. All the non-hydrogen atoms were refined anisotropically

for all the compounds. The H atoms attached to nitrogen in **1**, **2a** and **4a** were refined isotropically. Other hydrogen atoms were located at the calculated positions and refined as riding atoms. Table 1 summarizes the crystal data and refinement description.

4.5. Biological assays

4.5.1. Brine shrimps lethality assay

All the synthesized ligands and complexes were screened for their cytotoxicity by the brine shrimps lethality assay method with a little modification [44]. In short, stock solution of the test compounds was prepared (10 mg/ml of DMSO), artificial sea water with salt concentration 34 g/L in distilled H_2O was also prepared in which brine-shrimp (*Artemia salina*) eggs were hatched at room temperature, which were then transferred to vials containing sea water and final concentrations of test compounds (1000, 100 and 10 μg/ml) were obtained. After 24 h, the number of surviving shrimps was determined and LD_{50} was calculated by analyzing the data with the computer program Finny.

4.5.2. In vitro cytotoxicity screening

The test and reference compounds were dissolved to a concentration of 250,000 ng/ml in full medium, by a 20 fold dilution of a stock solution which contained 1 mg/200 μl. The compounds were taken into DMSO. *In vitro* cytotoxicity was estimated by the microculture sulforhodamine B (SRB) test [45]. The seven human cancer cell lines A498 (renal cancer), MCF-7 (estrogen receptor (ER)+/progesterone receptor (PgR)+ breast cancer), EVSA-T (estrogen receptor (ER)−/progesterone receptor (PgR) − breast cancer), H226 (lung cancer), IGROV (ovarian cancer), M19 MEL (melanoma) and WIDR (colon cancer), included in the anticancer screening panel of the National Cancer Institute, USA, were used in the present study.

The experiment was started on day 0. On day 0, 10,000 cells per well were seeded into 96-wells flat bottom microtiter plates (falcon 3072, DB). The plates were incubated overnight at 37 °C, 5% CO_2 to allow the cells to adhere to the bottom. On day 1, a three-fold dilution sequence of ten steps was made in full medium, starting with the 250,000 ng/mL stock solution. Every dilution was used in quadruplicate by adding 200 μl to a column of four wells. This procedure results in a highest concentration of 625,000 ng/ml present in column 1–2. Column 2 was used for the blank. After incubation of 3 days, the plates were washed with PBS (phosphate buffered saline) twice. The fluorescein diacetate (FDA) stock solution was diluted to 2 μg/ml with PBS and 200 μl of this solution was added to each of the control, experimental and blank wells. The plates were incubated for 30 min at 37 °C and the fluorescence generated from each well was measured at an excitation wavelength of 485 nm and an emission wavelength of 535 nm using an automated microplate reader (Labsystems Multiskan MS). Data was used for construction of concentration-response curves and determination of the ID_{50} value using the Deltasoft 3 software. The variability of the *in vitro* cytotoxicity test depends on *inter alia* the cell lines used and the serum applied. With the same batch of cell lines and the same batch of serum the inter-experimental CV (coefficient of variation) is 1–11% depending on the cell line and the intra-experimental CV is 2–4%. These values may be higher with other batches of cell lines and/or serum [46].

In vitro cytotoxicity data for complexes and reference compounds are given in Table 7.

4.5.3. In vitro antibacterial activity

Synthesized ligands and complexes were investigated for their antibacterial activity by the agar well diffusion method [47,48] against four strains of bacteria, two Gram positive, *S. aureus* (ATCC 6538), *M. luteus* (ATCC 10240) and two Gram negative, *E. coli* (ATCC 15224), *S. setubal* (ATCC 19196) strains. Cefixime and Roxithromycin were used as standard antibiotics.

An amount of 1 mg of the each compound was dissolved in 1 ml of DMSO. Nutrient agar medium was prepared by suspending nutrient agar (Merck) 2 g in 100 ml distilled water; pH 7.0, autoclaved, cooled and then seeded with 1 ml of prepared inoculum to have 10^6 CFU per ml. The Petri dishes were prepared by pouring 75 ml of seeded nutrient agar and allowed to solidify. Eleven wells per dish were made with sterile cork borer (8 mm), and labeled. Using a micropipette, 100 μl of test solutions were poured into the respective wells. Finally, the Petri dishes were incubated at 37 °C for 24 h. Triplicate plates were prepared for each sample. The diameter of the clear zone (showing no bacterial growth) around each well was measured with the help of vernier caliper. Antibacterial activities were calculated as a mean of 3 replicates.

4.5.4. Antifungal activity

The synthesized ligands and complexes were investigated for their antifungal activity against four fungal strains: *M. species* (*0300*), *A. niger* (*0198*), *Aspergillus flavus* (*0064*) and *F. solani* (*0291*). A susceptibility test was performed [49] with some modifications [50]. The samples were prepared in DMSO with concentration of 12 mg/ml. Sabouraud dextrose agar (Merck) was prepared in distilled water having the concentration of 65 g/L, pH was adjusted to 5.6, then autoclaved and cooled to 50 °C. A volume of 4 ml of this medium was poured into labeled test tubes and 67 μl of the each sample was added to the respective test tubes. The tubes were then allowed to solidify in a slanting position at room temperature. The tubes were prepared in triplicate for each fungus species. Other media supplemented with DMSO and reference antifungal drug (Terbinafine) were used as negative and positive controls, respectively. Each tube was inoculated with a 4 mm diameter piece of inoculum, removed from a seven days old culture of fungus. The tubes were incubated at 28 °C for 7 days. Cultures were examined twice weekly during the incubation. The growth in the medium was determined by measuring the linear growth (mm) and growth inhibition was calculated with reference to the negative control, using the following formula.

$$\text{Percentage inhibition of fungal growth} = 100 - \frac{\text{Linear growth in test(mm)}}{\text{Linear growth in control(mm)}} \times 100$$

Supplementary data

Crystallographic data (excluding structure factors) for the structures reported in this paper have been deposited to the Cambridge Crystallographic Data Centre as supplementary publication no. CCDC-815699 for **1**, CCDC-815700 for **2a** and CCDC-815698 for **4a**. Copies of available materials can be obtained, free of charge, on application to the director, CCDC, 12 Union Road, Cambridge CB21EZ, UK, (Fax: +44 (0) 1223 336033 or e-mail: deposit@ccdc.cam.ac.uk).

Acknowledgments

The authors are thankful to the Higher Education Commission of Pakistan for the grant of funds for the research project at Quaid-i-Azam University, Islamabad. The *in vitro* cytotoxicity screenings were carried out by Ms. P. F. Van Cuijk in the Laboratory of Transnational Pharmacology, Department of Medical Oncology, Erasmus Medical Center, Rotterdam, The Netherlands, under the supervision of Dr. E. A. C. Wiemer and Prof. G. Stoter.

Appendix. Supplementary data

Supplementary data associated with this article can be found in the online version, at doi:10.1016/j.ejmech.2011.11.029. These data include MOL files and InChiKeys of the most important compounds described in this article.

References

[1] V. Milacic, D. Chen, L. Ronconi, R. Kristin, L. Piwowar, D. Fregona, Q.P. Dou, Cancer Res. 66 (21) (2006) 10478–10486.
[2] (a) M. Gielen, E.R.T. Tiekink (Eds.), Metallotherapeutic Drugs and Metal-based Diagnostic Agents, John Wiley and Sons, Chichester, 2005;
(b) I. Kostova, Anti-Cancer Agents Med. Chem. 6 (2006) 19–32.
[3] (a) L. Ronconi, L. Giovagnini, C. Marzano, Inorg. Chem. 44 (2005) 1867–1881;
(b) L. Ronconi, C. Marzano, P. Zanello, J. Med. Chem. 49 (2006) 1648–1657.
[4] M.F. Ahmad, D. Singh, A. Taiyab, T. Ramakrishna, B. Raman, C.M. Rao, J. Mol. Biol. 382 (2008) 812–824.
[5] M.E. Letelier, A.M. Lepe, M. Faundez, J. Salazar, R. Marin, P. Aracena, H. Speisky, Chem. Biol. Interact 151 (2005) 71–82.
[6] H.W. Kuo, S.F. Chen, C.C. Wu, D.R. Chen, J.H. Lee, Biol. Trace Elem. Res. 89 (2002) 1–11.
[7] M.M. Eatock, A. Schatzlein, S.B. Kaye, Cancer Treat. Rev. 26 (2000) 191–204.
[8] E.J. Margalioth, J.G. Schenker, M. Chevion, Cancer 52 (1983) 868–872.
[9] S. Brem, Cancer Control 6 (1999) 436–458.
[10] J. Liu, H. Zhang, C. Chen, H. Deng, T. Lu, L. Ji, Dalton Trans. 1 (2003) 114–119.
[11] T.A. Khan, S. Naseem, S.N. Khan, A.U. Khan, M. Shakir, Spectrochim. Acta A 73 (2009) 622–629.
[12] R. Nagane, M. Chikira, M. Oumi, H. Shindo, W.E. Antholine, J. Inorg. Biochem. 78 (2000) 243–249.
[13] P. Gomez-Saiz, R. Gil-Garcia, M.A. Maestro, J.L. Pizarro, M.I. Arriortua, L. Lezama, T. Rojo, M. Gonzalez-Alvarez, J. Borras, J. Garcia-Tojal, J. Inorg. Biochem. 102 (2008) 1910–1920.
[14] P.R. Reddy, K.S. Rao, B. Satyanarayana, Tetrahedron Lett. 47 (2006) 7311–7315.
[15] F. Arjmand, B. Mohani, S. Ahmad, Eur. J. Med. Chem. 40 (2005) 1103–1110.
[16] A.P. Singh, N.K. Kaushik, A.K. Verma, G. Hundal, R. Gupta, Eur. J. Med. Chem. 44 (2009) 1607–1614.
[17] (a) X. Qiao, Z.Y. Ma, C.Z. Xie, F. Xue, Y.W. Zhang, J.Y. Xu, Z.Y. Qiang, J.S. Lou, G.J. Chen, S.P. Yan, J. Inorg. Biochem. 105 (2011) 728–737;
(b) G.J. Chen, X. Qiao, P.Q. Qiao, G.J. Xu, J.Y. Xu, J.L. Tian, W. Gu, X. Liu, S.P. Yan, J. Inorg. Biochem. 105 (2011) 119–126.
[18] (a) R.G.S. Berlinck, M.H. Kossuga, Nat. Prod. Rep. 22 (2005) 516–550;
(b) R.G.S. Berlinck, Nat. Prod. Rep. 19 (2002) 617–649;
(c) R.G.S. Berlinck, Nat. Prod. Rep. 13 (1996) 377–409;
(d) R.G.S. Berlinck, Nat. Prod. Rep. 16 (1999) 339–365.
[19] P.M. Fresneda, S. Delgado, A. Francesch, I. Manzanares, C. Cuevas, P. Molina, J. Med. Chem. 49 (2006) 1217–1221.
[20] (a) P.J. Hajduk, S. Boyd, D. Nettesheim, V. Nienaber, J. Severin, R. Smith, D. Davidson, T. Rockway, S.W. Fesik, J. Med. Chem. 43 (2000) 3862–3866;
(b) D.M. Evens, K. Sloanstakleff, M. Arvan, D.P. Guyton, Clin. Exp. Metastasis 16 (1998) 353–357;
(c) J. Jankun, R.W. Keck, E. Skrzypczak-Jankun, R. Swierca, Cancer Res. 57 (1997) 559–563.
[21] J. Chern, Y. Leu, S. Wang, R. Jou, S. Hsu, Y. Liaw, H. Lin, Med. Chem. 40 (1997) 2276–2286.
[22] (a) Z. Brzozowski, F. Saczewski, M. Gdaniec, Eur. J. Med. Chem. 37 (2002) 285–293;
(b) A.V. Dolzhenko, B.J. Tan, A.V. Dolzhenko, G.N.C. Chiu, W.K. Chui, J. Fluorine Chem. 129 (2008) 429–434.
[23] K. Ohara, M. Smietana, A. Restouin, S. Mollard, J. Borg, Y. Collette, J. Vasseur, J. Med. Chem. 50 (2007) 6465–6475.
[24] J.H. Chan, B. Roth, J. Med. Chem. 34 (1991) 550–555.
[25] (a) S. Cunha, M.B. Costa, H.B. Napolitano, C. Lauriucci, I. Vecanto, Tetrahedron 57 (2001) 1671–1675;
(b) U. Schröder, L. Beyer, R. Richter, J. Angulo-Cornejo, M. Castillo-Montoya, M. Lino-Pacheco, Inorg. Chim. Acta 353 (2003) 59–67.
[26] J. Binoy, C. James, I.H. Joe, V.S. Jayakumar, J. Mol. Str. 784 (2006) 32–46.
[27] S. Herres, A.J. Heuwing, U. Flörke, J. Schneider, G. Henkel, Inorg. Chim. Acta 358 (2005) 1089–1095.
[28] Atta-ur-Rahman, Nuclear Magnetic Resonance Spectroscopy, National Academy of Higher Education, Pakistan, 1989, 23–24.
[29] D.A. Powell, P.D. Ramsden, R.A. Batey, J. Org. Chem. 68 (2003) 2300–2309.
[30] (a) G. Murtaza, M. Said, M.K. Rauf, M. Ebihara, A. Badshah, Acta Cryst E63 (2007) o4664;
(b) G. Murtaza, Hanif-ur-Rehman, M.K. Rauf, M. Ebihara, A. Badshah, Acta Cryst E65 (2009) o343;
(c) G. Murtaza, M. Ebihara, M. Said, M.K. Rauf, S. Anwar, Acta Cryst E65 (2009) o2297–o2298.
[31] J. García-Tojal, A. García-Orad, J.L. Serra, J.L. Pizarro, L. Lezama, M.I. Arriortua, T. Rojo, J. Inorg. Biochem. 75 (1999) 45–54.
[32] J.L. McLaughlin, L.L. Rogers, Drug Inf. J. 32 (1998) 513–524.
[33] J.S. Metcalf, J. Lindsay, K.A. Beatie, S. Birmingham, M.L. Saker, A.K. Torokne, G.A. Codd, Toxicon 40 (2002) 1115–1120.
[34] (a) M.F. Primik, S. Göschl, M.A. Jacupek, A. Roller, B.K. Keppler, V.B. Arion, Inorg. Chem. 49 (2010) 11084–11095;
(b) A. Kellett, M. O'Connor, M. McCann, M. McNamara, P. Lynch, G. Rosair, V. McKee, B. Greaven, M. Walsh, S. McClean, A. Foltyn, D. O'Shea, O. Howe, M. Devereux, Dalton Trans. 40 (2011) 1024–1027.
[35] N. Dixit, R.K. Koiri, B.K. Mauya, S.K. Trgun, C. Höbartner, L. Mishra, J. Inorg. Biochem. 105 (2011) 256–267.
[36] S. Kashanian, M.M. Khodaei, H. Roshanfekr, N. Shahabadi, A. Rezvani, G. Mansouri, DNA Cell Biol. 30 (5) (2011) 287–296.
[37] Y. Zhang, J. Jiang, Y. Chen, Polymer 40 (1999) 6189–6198.
[38] R. Lakhan, B.P. Sharma, B.N. Shukla, Il Farmaco 55 (2000) 331–337.
[39] E. Rodriguez-Fernandez, J.L. Manzano, J.J. Benito, R. Hermosa, E. Monte, J.J. Criado, J. Inorg. Biochem. 99 (2005) 1558–1572.
[40] Atta-ur-Rahman, M.I. Choudhary, W.J. Thomesen, Bioassay Techniques for Drug Development, Harwood Academic Publishers, Amsterdam, 2001, 9–25.
[41] S.E. Blondelle, E. Crooks, J.M. Ostresh, R.A. Houghten, Antimicrob. Agents Chemother. 43 (1999) 106–114.
[42] A. Altomare, M.C. Burla, M. Camalli, G.L. Cascarano, C. Giacovazzo, A. Gaugliardi, A.G.G. Moliterni, G. Polidori, R. Spagna, J. Appl. Crystallogr. 32 (1999) 115–119.
[43] G.M. Sheldrick, SHELXL97, University of Gottingen, Germany, 1997.
[44] S. Inayatullah, R. Irum, A. Rehman, M.F. Chaudhary, B. Mirza, Pharm. Biol. 45 (2007) 397–403.
[45] Y.P. Keepers, P.E. Pizao, G.J. Peters, J. van Ark-Otte, B. Winograd, H.M. Pinedo, Eur. J. Cancer 27 (1991) 897–900.
[46] N. Katsaros, A. Anagnostopoulou, Crit. Rev. Oncol. Hematol. 42 (2002) 297–308.
[47] M.R. Boyd, Cancer Principles Pract. Oncol. 3 (1989) 1–12.
[48] B. Kivack, T. Mert, H. Tansel, Turk. J. Biol. 26 (2001) 197–200.
[49] R. Carran, A. Maran, J.M. Montero, L. Fernadozlago, A. Dominguez, Plants Med. Phyto. 21 (1987) 195–204.
[50] B.L. Lu, S.G. Zhang, Y.H. Zhang, Acta Pharm. Sin. 15 (1980) 118–123.